Rule-based Optimal Control for Autonomous Driving

Wei Xiao
Boston University
Brookline, MA
xiaowei@bu.edu

Noushin Mehdipour
Motional
Boston, MA
noushin.mehdipour@motional.com

Anne Collin
Motional
Boston, MA
anne.collin@motional.com

Amitai Bin-Nun
Motional
Boston, MA
amitai.binnun@motional.com

Emilio Frazzoli
Motional
Boston, MA
emilio.frazzoli@motional.com

Radboud Duintjer Tebbens
Motional
Boston, MA
radboud.tebbens@motional.com

Calin Belta
Motional
Boston, MA
calin.belta@motional.com

arXiv:2101.05709v1 [cs.RO] 14 Jan 2021

ABSTRACT

We develop optimal control strategies for Autonomous Vehicles (AVs) that are required to meet complex specifications imposed by traffic laws and cultural expectations of reasonable driving behavior. We formulate these specifications as rules, and specify their priorities by constructing a priority structure. We propose a recursive framework, in which the satisfaction of the rules in the priority structure are iteratively relaxed based on their priorities. Central to this framework is an optimal control problem, where convergence to desired states is achieved using Control Lyapunov Functions (CLFs), and safety is enforced through Control Barrier Functions (CBFs). We also show how the proposed framework can be used for after-the-fact, pass / fail evaluation of trajectories - a given trajectory is rejected if we can find a controller producing a trajectory that leads to less violation of the rule priority structure. We present case studies with multiple driving scenarios to demonstrate the effectiveness of the proposed framework.

CCS CONCEPTS

• **Computer systems organization** → **Robotic control**; • **Hardware** → *Safety critical systems*; • **Computing methodologies** → Computational control theory.

KEYWORDS

Autonomous driving, Lyapunov methods, Safety, Priority Structure

ACM Reference Format:
Wei Xiao, Noushin Mehdipour, Anne Collin, Amitai Bin-Nun, Emilio Frazzoli, Radboud Duintjer Tebbens, and Calin Belta. 2021. Rule-based Optimal Control for Autonomous Driving. In *ICCPS '21: 12th ACM/IEEE International Conference on Cyber-Physical Systems, May 19–21, 2021, Nashville, USA.* ACM, New York, NY, USA, 13 pages. https://doi.org/xxxx/xxxxxx

Permission to make digital or hard copies of all or part of this work for personal or classroom use is granted without fee provided that copies are not made or distributed for profit or commercial advantage and that copies bear this notice and the full citation on the first page. Copyrights for components of this work owned by others than ACM must be honored. Abstracting with credit is permitted. To copy otherwise, or republish, to post on servers or to redistribute to lists, requires prior specific permission and/or a fee. Request permissions from permissions@acm.org.
ICCPS '21, May 19–21, 2021, Nashville, USA
© 2021 Association for Computing Machinery.
ACM ISBN xxxx-xxxx…$15.00
https://doi.org/xxxx/xxxxxx

1 INTRODUCTION

With the development and integration of cyber physical and safety critical systems in various engineering disciplines, there is an increasing need for computational tools for verification and control of such systems according to rich and complex specifications. A prominent example is autonomous driving, which received a lot of attention during the last decade. Besides common objectives in optimal control problems, such as minimizing the energy consumption and travel time, and constraints on control variables, such as maximum acceleration, autonomous vehicles (AVs) should follow complex and possibly conflicting traffic laws with different priorities. They should also meet cultural expectations of reasonable driving behavior [5, 10, 16–18, 20, 23]. For example, an AV has to avoid collisions with other road users (high priority), drive faster than the minimum speed limit (low priority), and maintain longitudinal clearance with the lead car (medium priority). We formulate these behavior specifications as a set of rules with a priority structure that captures their importance [4].

To accommodate the rules, we formulate the AV control problem as an optimal control problem, in which the satisfaction of the rules and some vehicle limitations are enforced by Control Barrier Functions (CBF) [2], and convergence to desired states is achieved through Control Lyapunov Functions [8]. To minimize violation of the set of rules, we formulate iterative rule relaxation according to the pre-order on the rules.

Control Lyapunov Functions (CLFs) [3, 8] have been used to stabilize systems to desired states. CBFs enforce set forward-invariance [21, 25], and have been adopted to guarantee the satisfaction of safety requirements [2, 12, 24]. In [2, 9], the constraints induced by CBFs and CLFs were used to formulate quadratic programs (QPs) that could be solved in real time to stabilize affine control systems while optimizing quadratic costs and satisfying state and control constraints. The main limitation of this approach is that the resulting QPs can easily become infeasible, especially when

bounds on control inputs are imposed in addition to the safety specifications and the state constraints, or for constraints with high relative degree [26]. Relaxations of the (hard) CLF [1, 2] and CBF [26] constraints have been proposed to address this issue.

The approaches described above do not consider the (relative) importance of the safety constraints during their relaxations. With particular relevance to the application considered here, AVs often deal with situations where there are conflicts among some of the traffic laws or other requirements. For instance, consider a scenario where a pedestrian walks to the lane in which the AV is driving - it is impossible for the AV to avoid a collision with the pedestrian or another vehicles, stay in lane, and drive faster than the minimum speed limit at the same time. Given the relative priorities of these specifications, a reasonable AV behavior would be to avoid a collision with the pedestrian or other vehicles (high priority), and instead violate low or medium priority rules, e.g., by reducing speed to a value lower than the minimum speed limit, and/or deviating from its lane. The maximum satisfaction and minimum violation of a set of rules expressed in temporal logic were studied in [6, 22] and solved by assigning positive numerical weights to formulas based on their priorities [22]. In [4], the authors proposed *rulebooks*, a framework in which relative priorities were captured by a pre-order. In conjunction with rule violation scores, rulebooks were used to rank vehicle trajectories. These works do not consider the vehicle dynamics, or assume very simple forms, such as finite transition systems. The violation scores are example - specific, or are simply the quantitative semantics of the logic used to formulate the rules. In their current form, they capture worst case scenarios and are non-differentiable, and cannot be used for generating controllers for realistic vehicle dynamics.

In this paper, we draw inspiration from Signal Temporal Logic (STL) [13] to formalize traffic laws and other driving rules and to quantify the degree of violation of the rules by AV trajectories. We build on the rulebooks from [4] to construct a rule priority structure. The main contribution of this paper is an iterative procedure that uses the rule priority to determine a control strategy that minimizes rule violation globally. We show how this procedure can be adapted to develop transparent and reproducible rule-based pass/fail evaluation of AV trajectories in test scenarios. Central to these approaches is an optimization problem based on [26], which uses detailed vehicle dynamics, ensures the satisfaction of "hard" vehicle limitations (e.g., acceleration constraints), and can accommodate rule constraints with high relative degree. Another key contribution of this work is the formal definition of a speed dependent, optimal over-approximation of a vehicle footprint that ensures differentiability of clearance-type rules, which enables the use of powerful approaches based on CBF and CLF. Finally, we use and test the proposed architecture and algorithms were implemented in a user-friendly software tool in various driving scenarios.

2 PRELIMINARIES

2.1 Vehicle Dynamics

Consider an affine control system given by:

$$\dot{\boldsymbol{x}} = f(\boldsymbol{x}) + g(\boldsymbol{x})\boldsymbol{u}, \tag{1}$$

where $\boldsymbol{x} \in X \subset \mathbb{R}^n$ (X is the state constraint set), $\dot{()}$ denotes differentiation with respect to time, $f : \mathbb{R}^n \to \mathbb{R}^n$ and $g : \mathbb{R}^n \to \mathbb{R}^{n\times q}$ are globally Lipschitz, and $\boldsymbol{u} \in U \subset \mathbb{R}^q$, where U is the control constraint set defined as:

$$U := \{\boldsymbol{u} \in \mathbb{R}^q : \boldsymbol{u}_{min} \leq \boldsymbol{u} \leq \boldsymbol{u}_{max}\}, \tag{2}$$

with $\boldsymbol{u}_{min}, \boldsymbol{u}_{max} \in \mathbb{R}^q$, and the inequalities are interpreted componentwise. We use $\boldsymbol{x}(t)$ to refer to a trajectory of (1) at a specific time t, and we use $\mathcal{X}$ to denote a whole trajectory starting at time 0 and ending at a final time specified by a scenario. Note that most vehicle dynamics, such as "traditional" dynamics defined with respect to an inertial frame [2] and dynamics defined along a given reference trajectory [19] (see (18)) are in the form (1). Throughout the paper, we will refer to the vehicle with dynamics given by (1) as *ego*.

Definition 1. *(Forward invariance [15]) A set $C \subset \mathbb{R}^n$ is forward invariant for system (1) if $\boldsymbol{x}(0) \in C$ implies $\boldsymbol{x}(t) \in C$, $\forall t \geq 0$.*

Definition 2. *(Relative degree [15]) The relative degree of a (sufficiently many times) differentiable function $b : \mathbb{R}^n \to \mathbb{R}$ with respect to system (1) is the number of times it needs to be differentiated along its dynamics (Lie derivatives) until the control $\boldsymbol{u}$ explicitly shows in the corresponding derivative.*

In this paper, since function b is used to define a constraint $b(\boldsymbol{x}) \geq 0$, we will also refer to the relative degree of b as the relative degree of the constraint.

2.2 High Order Control Barrier Functions

Definition 3. *(Class $\mathcal{K}$ function [11]) A continuous function $\alpha : [0, a) \to [0, \infty), a > 0$ is said to belong to class $\mathcal{K}$ if it is strictly increasing and $\alpha(0) = 0$.*

Given $b : \mathbb{R}^n \to \mathbb{R}$ and a constraint $b(\boldsymbol{x}) \geq 0$ with relative degree m, we define $\psi_0(\boldsymbol{x}) := b(\boldsymbol{x})$ and a sequence of functions $\psi_i : \mathbb{R}^n \to \mathbb{R}, i \in \{1, \dots, m\}$:

$$\psi_i(\boldsymbol{x}) := \dot{\psi}_{i-1}(\boldsymbol{x}) + \alpha_i(\psi_{i-1}(\boldsymbol{x})), i \in \{1, \dots, m\}, \tag{3}$$

where $\alpha_i(\cdot), i \in \{1, \dots, m\}$ denotes a $(m-i)^{th}$ order differentiable class $\mathcal{K}$ function. We further define a sequence of sets $C_i, i \in \{1, \dots, m\}$ associated with (3) in the following form:

$$C_i := \{\boldsymbol{x} \in \mathbb{R}^n : \psi_{i-1}(\boldsymbol{x}) \geq 0\}, i \in \{1, \dots, m\}. \tag{4}$$

Definition 4. *(High Order Control Barrier Function (HOCBF) [26]) Let $C_1, \dots, C_m$ be defined by (4) and $\psi_1(\boldsymbol{x}), \dots, \psi_m(\boldsymbol{x})$ be defined by (3). A function $b : \mathbb{R}^n \to \mathbb{R}$ is a High Order Control Barrier Function (HOCBF) of relative degree m for system (1) if there exist $(m-i)^{th}$ order differentiable class $\mathcal{K}$ functions $\alpha_i, i \in \{1, \dots, m-1\}$ and a class $\mathcal{K}$ function α_m such that*

$$\sup_{\boldsymbol{u}\in U} [L_f^m b(\boldsymbol{x}) + L_g L_f^{m-1} b(\boldsymbol{x})\boldsymbol{u} + S(b(\boldsymbol{x})) + \alpha_m(\psi_{m-1}(\boldsymbol{x}))] \geq 0, \tag{5}$$

for all $\boldsymbol{x} \in C_1 \cap, \dots, \cap C_m$. L_f^m (L_g) denotes Lie derivatives along f (g) m (one) times, and $S(\cdot)$ denotes the remaining Lie derivatives along f with degree less than or equal to $m-1$ (see [26] for more details).

The HOCBF is a general form of the relative degree 1 CBF [2], [9], [12] (setting $m = 1$ reduces the HOCBF to the common CBF form in [2], [9], [12]), and is also a general form of the exponential CBF [15].

Theorem 1. *([26]) Given a HOCBF $b(\boldsymbol{x})$ from Def. 4 with the associated sets $C_1, \ldots, C_m$ defined by (4), if $\boldsymbol{x}(0) \in C_1 \cap, \ldots, \cap C_m$, then any Lipschitz continuous controller $\boldsymbol{u}(t)$ that satisfies (5) $\forall t \geq 0$ renders $C_1 \cap, \ldots, \cap C_m$ forward invariant for system (1).*

Definition 5. *(Control Lyapunov Function (CLF) [1]) A continuously differentiable function $V : \mathbb{R}^n \to \mathbb{R}_{\geq 0}$ is an exponentially stabilizing control Lyapunov function (CLF) if there exist positive constants $c_1 > 0, c_2 > 0, c_3 > 0$ such that $\forall \boldsymbol{x} \in X$, $c_1||\boldsymbol{x}||^2 \leq V(\boldsymbol{x}) \leq c_2||\boldsymbol{x}||^2$, the following holds:*

$$\inf_{\boldsymbol{u} \in U} [L_f V(\boldsymbol{x}) + L_g V(\boldsymbol{x})\boldsymbol{u} + c_3 V(\boldsymbol{x})] \leq 0. \tag{6}$$

Theorem 2 ([1]). *Given a CLF as in Def. 5, any Lipschitz continuous controller $\boldsymbol{u}(t), \forall t \geq 0$ that satisfies (6) exponentially stabilizes system (1) to the origin.*

Recent works [2],[12],[15] combined CBFs and CLFs with quadratic costs to formulate an optimization problem that stabilized a system using CLFs subject to safety constraints given by CBFs. In this work, we follow a similar approach. Time is discretized and CBFs and CLFs constraints are considered at each discrete time step. Note that these constraints are linear in control since the state value is fixed at the beginning of the discretization interval. Therefore, in every interval, the optimization problem is a QP . The optimal control obtained by solving each QP is applied at the current time step and held constant for the whole interval. The next state is found by integrating the dynamics (1). The usefulness of this approach is conditioned upon the feasibility of the QP at every time step. In the case of constraints with high relative degrees, which are common in autonomous driving, the CBFs can be replaced by HOCBFs.

2.3 Rulebooks

As defined in [4], a *rule* specifies a desired behavior for autonomous vehicles. Rules can be derived from traffic laws, local culture, or consumer expectation, e.g., "stay in lane for all times", "maintain clearance from pedestrians for all times", "obey the maximum speed limit for all times", "reach the goal". A *rulebook* as introduced in [4] defines a priority on rules by imposing a pre-order that can be used to rank AV trajectories:

Definition 6. *(Rulebook [4]) A rulebook is a tuple $\langle R, \leq \rangle$, where R is a finite set of rules and $\leq$ is a pre-order on R.*

A rulebook can be represented by a directed graph, where each node is a rule and an edge between two rules means that the first rule has higher priority than the second. Formally, $r_1 \to r_2$ in the graph means that $r_1 \leq r_2$ ($r_2 \in R$ has a higher priority than $r_1 \in R$). Note that, using a pre-order, two rules can be in one of three relations: comparable (one has a higher priority than the other), incomparable, or equivalent (each has a higher priority than the other).

Example 1. *Consider the rulebook shown in Fig. 1, which consists of 6 rules. In this example, r_1 and r_2 are incomparable, and both have a higher priority than r_3 and r_4. Rules r_3 and r_4 are equivalent ($r_3 \leq r_4$ and $r_4 \leq r_3$), but are incomparable to r_5. Rule r_6 has the lowest priority among all rules.*

Rules are evaluated over vehicle trajectories (i.e., trajectories of system (1)). A *violation metric* is a function specific to a rule that takes as input a trajectory and outputs a *violation score* that captures the degree of violation of the rule by the trajectory [4]. For example, if the AV crosses the lane divider and reaches within the left lane by a maximum distance of 1m along a trajectory, then the violation score for that trajectory against the "stay in lane for all times" rule can be 1m.

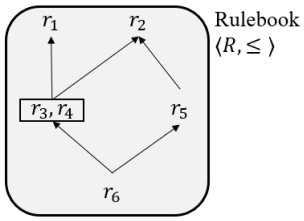


Figure 1: Graphical representation of a rulebook $\langle R, \leq \rangle$.

3 PROBLEM FORMULATION

For a vehicle with dynamics given by (1) and starting at a given state $\boldsymbol{x}(0) = \boldsymbol{x}_0$, consider an optimal control problem in the form:

$$\min_{\boldsymbol{u}(t)} \int_0^T J(||\boldsymbol{u}(t)||)dt, \tag{7}$$

where $||\cdot||$ denotes the 2-norm of a vector, $T > 0$ denotes a bounded final time, and J is a strictly increasing function of its argument (e.g., an energy consumption function $J(||\boldsymbol{u}(t)||) = ||\boldsymbol{u}(t)||^2$). We consider the following additional requirements:

Trajectory tracking: We require the vehicle to stay as close as possible to a desired *reference trajectory* $\mathcal{X}_r$ (e.g., middle of its current lane).

State constraints: We impose a set of constraints (componentwise) on the state of system (1) in the following form:

$$\boldsymbol{x}_{min} \leq \boldsymbol{x}(t) \leq \boldsymbol{x}_{max}, \forall t \in [0, T], \tag{8}$$

where $\boldsymbol{x}_{max} := (x_{max,1}, x_{max,2}, \ldots, x_{max,n}) \in \mathbb{R}^n$ and $\boldsymbol{x}_{min} := (x_{min,1}, x_{min,2}, \ldots, x_{min,n}) \in \mathbb{R}^n$ denote the maximum and minimum state vectors, respectively. Examples of such constraints for a vehicle include maximum acceleration, maximum braking, and maximum steering rate.

Priority structure: We require the system trajectory $\mathcal{X}$ of (1) starting at $\boldsymbol{x}(0) = \boldsymbol{x}_0$ to satisfy a priority structure $\langle R, \sim_p, \leq_p \rangle$, i.e.:

$$\mathcal{X} \models \langle R, \sim_p, \leq_p \rangle, \tag{9}$$

where $\sim_p$ is an equivalence relation over a finite set of rules R and $\leq_p$ is a total order over the equivalence classes. Our priority structure is related to the rulebook from Sec. 2.3, but it requires that any two rules from R are either comparable or equivalent (see Sec. 4.2 for a formal definition). Informally, this means that $\mathcal{X}$ is the "best" trajectory that (1) can produce, considering the violation metrics of the rules in R and the priorities captured by $\sim_p$ and $\leq_p$. A formal definition for a priority structure and its satisfaction will be given in Sec. 4.2.

Control bounds: We impose control bounds as given in (2). Examples include jerk and steering acceleration.

Formally, we can define the optimal control problem as follows:

Problem 1. *Find a control policy for system (1) such that the objective function in (7) is minimized, and the trajectory tracking,*

state constraints (8), priority structure $\langle R, \sim_p, \leq_p \rangle$, and control bounds (2) are satisfied by the generated trajectory given $\boldsymbol{x}(0)$.

Our approach to Problem 1 can be summarized as follows: We use CLFs for tracking the reference trajectory $\mathcal{X}_r$ and HOCBFs to implement the state constraints (8). For each rule in R, we define violation metrics. We show that satisfaction of the rules can be written as forward invariance for sets described by differential functions, and enforce them using HOCBFs. The control bounds (2) are considered as constraints. We provide an iterative solution to Problem 1, where each iteration involves solving a sequence of QPs. In the first iteration, all the rules from R are considered. If the corresponding QPs are feasible, then an optimal control is found. Otherwise, we iteratively relax the satisfaction of rules from subsets of R based on their priorities, and minimize the corresponding relaxations by including them in the cost function.

4 RULES AND PRIORITY STRUCTURES

In this section, we extend the rulebooks from [4] by formalizing the rules and defining violation metrics. We introduce a *priority structure*, in which all rules are comparable, and it is particularly suited for the hierarchical control framework proposed in Sec. 5.3.

4.1 Rules

In the definition below, an *instance $i \in S_p$* is a traffic participant or artifact that is involved in a rule, where S_p is the set of all instances involved in the rule. For example, in a rule to maintain clearance from pedestrians, a pedestrian is an instance, and there can be many instances encountered by ego in a given scenario. Instances can also be traffic artifacts like the road boundary (of which there is only one), lane boundaries, or stop lines.

Definition 7. *(Rule) A rule is composed of a statement and three violation metrics. A statement is a formula that is required to be satisfied for all times. A formula is inductively defined as:*

$$\varphi := \mu | \neg\varphi | \varphi_1 \wedge \varphi_2, \tag{10}$$

where $\varphi, \varphi_1, \varphi_2$ are formulas, $\mu := (h(\boldsymbol{x}) \geq 0)$ is a predicate on the state vector $\boldsymbol{x}$ of system (1) with $h : \mathbb{R}^n \to \mathbb{R}$. $\wedge, \neg$ are Boolean operators for conjunction and negation, respectively. The three violation metrics for a rule r are defined as:

1. *instantaneous violation metric $\varrho_{r,i}(\boldsymbol{x}(t)) \in [0, 1]$,*
2. *instance violation metric $\rho_{r,i}(\mathcal{X}) \in [0, 1]$, and*
3. *total violation metric $P_r(\mathcal{X}) \in [0, 1]$,*

where i is an instance, $\boldsymbol{x}(t)$ is a trajectory at time t and $\mathcal{X}$ is a whole trajectory of ego. The instantaneous violation metric $\varrho_{r,i}(\boldsymbol{x}(t))$ quantifies violation by a trajectory at a specific time t with respect to a given instant i. The instance violation metric $\rho_{r,i}(\mathcal{X})$ captures violation with respect to a given instance i over the whole time of a trajectory, and is obtained by aggregating $\varrho_{r,i}(\boldsymbol{x}(t))$ over the entire time of a trajectory $\mathcal{X}$. The total violation metric P_r is the aggregation of the instance violation metric $\rho_{r,i}(\mathcal{X})$ over all instances $i \in S_p$.

The aggregations in the above definitions can be implemented through selection of a maximum or a minimum, integration over time, summation over instances, or by using general L_p norms. A zero value for a violation score shows satisfaction of the rule. A strictly positive value denotes violation - the larger the score, the more ego violates the rule. Throughout the paper, for simplicity, we use ϱ_r and ρ_r instead of $\varrho_{r,i}$ and $\rho_{r,i}$ if there is only one instance. Examples of rules (statements and violations metrics and scores) are given in Sec. 6 and in the Appendix.

We divide the set of rules into two categories: (1) *clearance rules* - safety relevant rules enforcing that ego maintains a minimal distance to other traffic participants and to the side of the road or lane (2) *non-clearance rules* - rules that that are not contained in the first category, such as speed limit rules. In Sec. 5.2, we provide a general methodology to express clearance rules as inequalities involving differentiable functions, which will allow us to enforce their satisfaction using HOCBFs.

Remark 1. *The violation metrics from Def. 7 are inspired from Signal Temporal Logic (STL) robustness [7, 13, 14], which quantifies how a signal (trajectory) satisfies a temporal logic formula. In this paper, we focus on rules that we aim to satisfy for all times. Therefore, the rules in (10) can be seen as (particular) STL formulas, which all start with an "always" temporal operator (omitted here).*

4.2 Priority Structure

The pre-order rulebook in Def. 6 defines a "base" pre-order that captures relative priorities of some (comparable) rules, which are often similar in different states and countries. A pre-order rulebook can be made more precise for a specific legislation by adding rules and/or priority relations through priority refinement, rule aggregation and augmentation [4]. This can be done through empirical studies or learning from local data to construct a total order rulebook. To order trajectories, authors of [4] enumerated all the total orders compatible with a given pre-order. In this paper, motivated by the hierarchical control framework described in Sec. 5.3, we require that any two rules are in a relationship, in the sense that they are either equivalent or comparable with respect to their priorities.

Definition 8 (Priority Structure). *A priority structure is a tuple $\langle R, \sim_p, \leq_p \rangle$, where R is a finite set of rules, $\sim_p$ is an equivalence relation over R, and $\leq_p$ is a total order over the set of equivalence classes determined by $\sim_p$.*

Equivalent rules (i.e., rules in the same class) have the same priority. Given two equivalence classes O_1 and O_2 with $O_1 \leq_p O_2$, every rule $r_1 \in O_1$ has lower priority than every rule $r_2 \in O_2$. Since $\leq_p$ is a total order, any two rules $r_1, r_2 \in R$ are comparable, in the sense that exactly one of the following three statements is true: (1) r_1 and r_2 have the same priority, (2) r_1 has higher priority than r_2, and (3) r_2 has higher priority than r_1. Given a priority structure $\langle R, \sim_p, \leq_p \rangle$, we can assign numerical (integer) priorities to the rules. We assign priority 1 to the equivalence class with the lowest priority, priority 2 to the next one and so on. The rules inside an equivalence class inherit the priority from their equivalence class. Given a priority structure $\langle R, \sim_p, \leq_p \rangle$ and violation scores for the rules in R, we can compare trajectories:

Definition 9 (Trajectory Comparison). *A trajectory $\mathcal{X}_1$ is said to be* **better** *(less violating) than another trajectory $\mathcal{X}_2$ if the highest priority rule(s) violated by $\mathcal{X}_1$ has a lower priority than the highest priority rule(s) violated by $\mathcal{X}_2$. If both trajectories violate an equivalent highest priority rule(s), then the one with the smaller (maximum)*

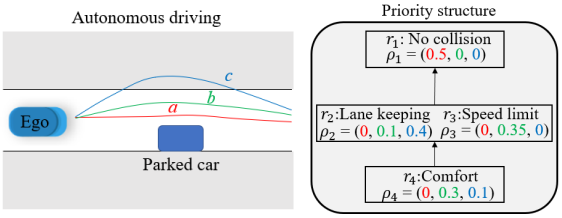
total violation score is better. In this case, if the trajectories have equal violation scores, then they are equivalent.

It is easy to see that, by following Def. 9, given two trajectories, one can be better than the other, or they can be equivalent (i.e., two trajectories cannot be incomparable).

Example 2. *Consider the driving scenario from Fig. 2(a) and a priority structure* $\langle R, \sim_p, \leq_p \rangle$ *in Fig. 2(b), where* $R = \{r_1, r_2, r_3, r_4\}$, *and* r_1*: "No collision",* r_2*: "Lane keeping",* r_3*: "Speed limit" and* r_4*: "Comfort". There are 3 equivalence classes given by* $O_1 = \{r_4\}$, $O_2 = \{r_2, r_3\}$ *and* $O_3 = \{r_1\}$. *Rule* r_4 *has priority 1,* r_2 *and* r_3 *have priority 2, and* r_1 *has priority 3. Assume the instance (same as total, as there is only one instance for each rule) violation scores of rule* $r = 1, 2, 3, 4$ *by trajectories* a, b, c *are given by* $\rho_r = (\rho_r(a), \rho_r(b), \rho_r(c))$ *as shown in Fig. 2(b). Based on Def. 9, trajectory* c *is better (less violating) than trajectory* a *since the highest priority rule violated by* c *(*r_2*) has a lower priority than the highest priority rule violated by* a *(*r_1*). The same argument holds for trajectories* a *and* b*, i.e.,* b *is better than* a*. The highest priority rules violated by trajectories* b *and* c *have the same priorities. Since the maximum violation score of the highest priority rules violated by* b *is smaller than that for* c*, i.e.,* $\max(\rho_2(b), \rho_3(b)) = 0.35$, $\max(\rho_2(c), \rho_3(c)) = 0.4$, *trajectory* b *is better than* c.

Definition 10. *(Priority structure satisfaction) A trajectory* $\mathcal{X}$ *of system (1) starting at* $\boldsymbol{x}(0)$ *satisfies a priority structure* $\langle R, \sim_p, \leq_p \rangle$ *(i.e.,* $\mathcal{X} \models \langle R, \sim_p, \leq_p \rangle$*), if there are no better trajectories of (1) starting at* $\boldsymbol{x}(0)$.

Def. 10 is central to our solution to Problem 1 (see Sec. 5.3), which is based on an iterative relaxation of the rules according to their satisfaction of the priority structure.



(a) Possible trajectories

(b) Priority structure with instance violation scores (the colors for the scores correspond to the colors of the trajectories. The rectangles show the equivalence classes.

Figure 2: An autonomous driving scenario with three possible trajectories, 4 rules, and 3 equivalence classes

5 RULE-BASED OPTIMAL CONTROL

In this section, we present our approach to solve Problem 1.

5.1 Trajectory Tracking

As discussed in Sec. 2.1, Eqn. (1) can define "traditional" vehicle dynamics with respect to an inertial reference frame [2], or dynamics defined along a given reference trajectory [19] (see (18)). The case study considered in this paper falls in the second category (the middle of ego's current lane is the default reference trajectory). We use the model from [19], in which part of the state of (1) captures the tracking errors with respect to the reference trajectory. The tracking problem then becomes stabilizing the error states to 0. Suppose the error state vector is $\boldsymbol{y} \in R^{n_0}$, $n_0 \leq n$ (the components in $\boldsymbol{y}$ are part of the components in $\boldsymbol{x}$). We define a CLF $V(\boldsymbol{x}) = ||\boldsymbol{y}||^2$ ($c_3 = \epsilon > 0$ in Def. 5). Any control $\boldsymbol{u}$ that satisfies the relaxed CLF constraint [2] given by:

$$L_f V(\boldsymbol{x}) + L_g V(\boldsymbol{x})\boldsymbol{u} + \epsilon V(\boldsymbol{x}) \leq \delta_e, \tag{11}$$

exponentially stabilizes the error states to 0 if $\delta_e(t) = 0, \forall t \in [0, T]$, where $\delta_e > 0$ is a relaxation variable that compromises between stabilization and feasibility. Note that the CLF constraint (11) only works for $V(\boldsymbol{x})$ with relative degree one. If the relative degree is larger than 1, we can use input-to-state linearization and state feedback control [11] to reduce the relative degree to one [27].

5.2 Clearance and Optimal Disk Coverage

Satisfaction of a priority structure can be enforced by formulating real-time constraints on ego state $\boldsymbol{x}(t)$ that appear in the violation metrics. Satisfaction of the non-clearance rules can be easily implemented using HOCBFs (See Sec. 5.3, Sec. A). For clearance rules, we define a notion of clearance region around ego and around the traffic participants in S_p that are involved in the rule (e.g., pedestrians and other vehicles). The clearance region for ego is defined as a rectangle with tunable speed-dependent lengths (i.e., we may choose to have a larger clearance from pedestrians when ego is driving with higher speeds) and defined based on ego footprint and functions $h_f(\boldsymbol{x}), h_b(\boldsymbol{x}), h_l(\boldsymbol{x}), h_r(\boldsymbol{x})$ that determine the front, back, left, and right clearances as illustrated in Fig. 3, where $h_f, h_b, h_l, h_r : \mathbb{R}^n \to \mathbb{R}_{\geq 0}$. The clearance regions for participants (instances) are defined such that they comply with their geometry and cover their footprints, e.g., (fixed-length) rectangles for other vehicles and (fixed-radius) disks for pedestrians, as shown in Fig. 3.

To satisfy a clearance rule involving traffic participants, we need to avoid any overlaps between the clearance regions of ego and traffic participants. We define a function $d_{min}(\boldsymbol{x}, \boldsymbol{x}_i) : \mathbb{R}^{n+n_i} \to \mathbb{R}$ to determine the signed distance between the clearance regions of ego and participant $i \in S_p$ ($\boldsymbol{x}_i \in \mathbb{R}^{n_i}$ denotes the state of participant i), which is negative if the clearance regions overlap. Therefore, satisfaction of a clearance rule can be imposed by having a constraint on $d_{min}(\boldsymbol{x}, \boldsymbol{x}_i)$ to be non-negative. For the clearance rules "stay in lane" and "stay in drivable area", we require that ego clearance region be within the lane and the drivable area, respectively.

However, finding $d_{min}(\boldsymbol{x}, \boldsymbol{x}_i)$ can be computationally expensive. For example, the distance between two rectangles could be from corner to corner, corner to edge, or edge to edge. Since each rectangle has 4 corners and 4 edges, there are 64 possible cases. More importantly, this computation leads to a non-smooth $d_{min}(\boldsymbol{x}, \boldsymbol{x}_i)$ function, which cannot be used to enforce clearance using a CBF approach. To address these issues, we propose an optimal coverage of the rectangles with disks, which allows to map the satisfaction of the clearance rules to a set of smooth HOCBF constraints (i.e., there will be one constraint for each pair of centers of disks pertaining to different traffic participants).

We use $l > 0$ and $w > 0$ to denote the length and width of ego's footprint, respectively. Assume we use $z \in \mathbb{N}$ disks with centers located on the center line of the clearance region to cover it (see Fig. 4). Since all the disks have the same radius, the minimum radius to fully cover ego's clearance region, denoted by $\mathfrak{r} > 0$, is given by:

$$\mathfrak{r} = \sqrt{\left(\frac{w + h_l(\boldsymbol{x}) + h_r(\boldsymbol{x})}{2}\right)^2 + \left(\frac{l + h_f(\boldsymbol{x}) + h_b(\boldsymbol{x})}{2z}\right)^2}. \quad (12)$$

The minimum radius $\mathfrak{r}_i$ of the rectangular clearance region for a traffic participant $i \in S_p$ with disks number z_i is defined in a similar way using the length and width of its footprint and setting $h_l, h_r, h_b, h_f = 0$.

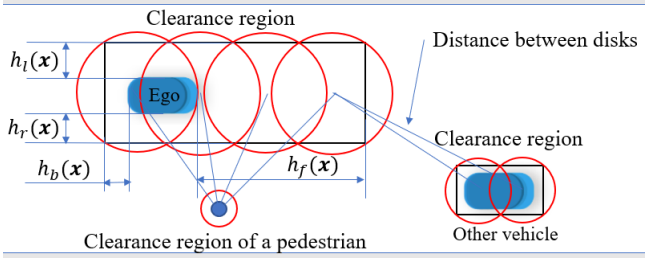


Figure 3: The clearance regions and their coverage with disks: the clearance region and the disks are speed dependent for ego and fixed for the other vehicle and the pedestrian. We consider the distances between all the possible pairs of disks from ego and other traffic participants (vehicles, pedestrians, etc.).

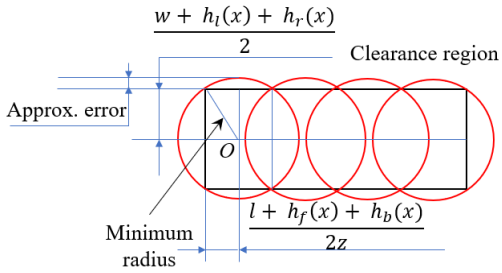


Figure 4: The optimal disk coverage of a clearance region.

Assume the center of the disk $j \in \{1, \dots, z\}$ for ego, and the center of the disk $k \in \{1, \dots, z_i\}$ for the instance $i \in S_p$ are given by $(x_{e,j}, y_{e,j}) \in \mathbb{R}^2$ and $(x_{i,k}, y_{i,k}) \in \mathbb{R}^2$, respectively (See Appendix B). To avoid any overlap between the corresponding disks of ego and the instance $i \in S_p$, we impose the following constraints:

$$\sqrt{(x_{e,j} - x_{i,k})^2 + (y_{e,j} - y_{i,k})^2} \geq \mathfrak{r} + \mathfrak{r}_i, \quad \forall j \in \{1, \dots, z\}, \forall k \in \{1, \dots, z_i\}. \quad (13)$$

Since disks fully cover the clearance regions, enforcing (13) also guarantees that $d_{min}(\boldsymbol{x}, \boldsymbol{x}_i) \geq 0$. For the clearance rules "stay in lane" and "stay in drivable area", we can get similar constraints as (13) to make the disks that cover ego's clearance region stay within them (e.g., we can consider $h_l, h_r, h_b, h_f = 0$ and formulate (13) such that the distance between ego disk centers and the line in the middle of ego's current lane be less than $\frac{w}{2} - \mathfrak{r}$). Thus, we can formulate satisfaction of all the clearance rules as continuously differentiable constraints (13), and implement them using HOCBFs.

To efficiently formulate the proposed optimal disk coverage approach, we need to find the minimum number of the disks that fully cover the clearance regions as it determines the number of constraints in (13). Moreover, we need to minimize the lateral approximation error since large errors imply overly conservative constraint (See Fig. 4). This can be formally defined as an optimization problem, and solved offline to determine the numbers and radii of the disks in (13) (the details are provided in Appendix B).

5.3 Optimal Control

In this section, we present our complete framework to solve Problem 1. We propose a recursive algorithm to iteratively relax the satisfaction of the rules in the priority structure $\langle R, \sim_p, \leq_p \rangle$ (if needed) based on the total order over the equivalence classes.

Let R_O be the set of equivalence classes in $\langle R, \sim_p, \leq_p \rangle$, and N_O be the cardinality of R_O. We construct the power set of equivalence classes denoted by $S = 2^{R_O}$, and incrementally (from low to high priority) sort the sets in S based on the highest priority of the equivalence classes in each set according to the total order and denote the sorted set by $S_{sorted} = \{S_1, S_2, \dots, S_{2^{N_O}}\}$, where $S_1 = \{\emptyset\}$. We use this sorted set in our optimal control formulation to obtain satisfaction of the higher priority classes, even at the cost of relaxing satisfaction of the lower priority classes. Therefore, from Def. 10, the solution of the optimal control will satisfy the priority structure.

Example 3. *Reconsider Exm. 2. We define $R_O = \{O_1, O_2, O_3\}$. Based on the given total order $O_1 \leq_p O_2 \leq_p O_3$, we can write the sorted power set as $S_{sorted} = \{\{\emptyset\}, \{O_1\}, \{O_2\}, \{O_1, O_2\}, \{O_3\}, \{O_1, O_3\}, \{O_2, O_3\}, \{O_1, O_2, O_3\}\}$.*

In order to find a trajectory that satisfies a given priority structure, we first assume that all the rules are satisfied. Starting from $S_1 = \{\emptyset\}$ in the sorted set S_{sorted}, we solve Problem 1 given that no rules are relaxed, i.e., all the rules must be satisfied. If the problem is infeasible, we move to the next set $S_2 \in S_{sorted}$, and relax all the rules of all the equivalence classes in S_2 while enforcing satisfaction of all the other rules in the equivalence class set denoted by $R_O \setminus S_2$. This procedure is done recursively until we find a feasible solution of Problem 1. Formally, at $k = 1, 2 \dots, 2^{N_O}$ for $S_k \in S_{sorted}$, we relax all the rules $i \in O$ for all the equivalence classes $O \in S_k$ and reformulate Problem 1 as the following optimal control problem:

$$\min_{\boldsymbol{u}, \delta_e, \delta_{i, i \in S_k}} \int_0^T J(||\boldsymbol{u}||) + p_e \delta_e^2 + \sum_{i \in S_k} p_i \delta_i^2 dt \quad (14)$$

subject to:

dynamics (1), control bounds (2), CLF constraint (11),

$$L_f^{m_j} b_j(\boldsymbol{x}) + L_g L_f^{m_j-1} b_j(\boldsymbol{x})\boldsymbol{u} + S(b_j(\boldsymbol{x})) + \alpha_{m_j}(\psi_{m_j-1}(\boldsymbol{x})) \geq 0, \forall j \in O, \forall O \in R_O \setminus S_k, \tag{15}$$

$$L_f^{m_i} b_i(\boldsymbol{x}) + L_g L_f^{m_i-1} b_i(\boldsymbol{x})\boldsymbol{u} + S(b_i(\boldsymbol{x})) + \alpha_{m_i}(\psi_{m_i-1}(\boldsymbol{x})) \geq \delta_i, \forall i \in O, \forall O \in S_k, \tag{16}$$

$$L_f^{m_l} b_l(\boldsymbol{x}) + L_g L_f^{m_l-1} b_{lim,l}(\boldsymbol{x})\boldsymbol{u} + S(b_{lim,l}(\boldsymbol{x})) + \alpha_{m_l}(\psi_{m_l-1}(\boldsymbol{x})) \geq 0, \forall l \in \{1, \ldots, 2n\}, \tag{17}$$

where $p_e > 0$ and $p_i > 0, i \in S_k$ assign the trade-off between the the CLF relaxation δ_e (used for trajectory tracking) and the HOCBF relaxations δ_i. m_i, m_j, m_l denotes the relative degree of $b_i(\boldsymbol{x}), b_j(\boldsymbol{x}), b_{lim,l}(\boldsymbol{x})$, respectively. The functions $b_i(\boldsymbol{x})$ and $b_j(\boldsymbol{x})$ are HOCBFs for the rules in $\langle R, \sim_p, \leq_p \rangle$, and are implemented directly from the rule statement for non-clearance rules or by using the optimal disk coverage framework for clearance rules. At relaxation step k, HOCBFs corresponding to the rules in $O, \forall O \in S_k$ are relaxed by adding $p_i > 0, i \in S_k$ in (15), while for other rules in R in (16) and the state constraints (17), regular HOCBFs are used. We assign $p_i, i \in S_k$ according to their relative priorities, i.e., we choose a larger p_i for the rule i that belongs to a higher priority class. The functions $b_{lim,l}(\boldsymbol{x}), l \in \{1, \ldots, 2n\}$ are HOCBFs for the state limitations (8). The functions $\psi_{m_i}(\boldsymbol{x}), \psi_{m_j}(\boldsymbol{x}), \psi_{m_l}(\boldsymbol{x})$ are defined as in (3). $\alpha_{m_i}, \alpha_{m_j}, \alpha_{m_l}$ can be penalized to improve the feasibility of the problem above [26, 28].

If the above optimization problem is feasible for all $t \in [0, T]$, we can specifically determine which rules (within an equivalence class) are relaxed based on the values of $\delta_i, i \in O, O \in S_k$ in the optimal solution (i.e., if $\delta_i(t) = 0, \forall t \in \{0, T\}$, then rule i does not need to be relaxed). This procedure is summarized in Alg. 1.

Remark 2 (Complexity). *The optimization problem (14) is solved using QPs introduced in Sec. 2. The complexity of the QP is $O(y^3)$, where $y \in \mathbb{N}$ is the dimension of decision variables. It usually takes less than 0.01s to solve each QP in Matlab. The total time for each iteration $k \in \{1, \ldots, 2^{N_O}\}$ depends on the final time T and the length of the reference trajectory $\mathcal{X}_r$. The computation time can be further improved by running the code in parallel over multiple processors.*

5.4 Pass/Fail Evaluation

As an extension to Problem 1, we formulate and solve a pass / fail (P/F) procedure, in which we are given a vehicle trajectory, and the goal is to accept (pass, P) or reject (fail, F) it based on the satisfaction of the rules. Specifically, given a candidate trajectory $\mathcal{X}_c$ of system (1), and given a priority structure $\langle R, \sim_p, \leq_p \rangle$, we pass (P) $\mathcal{X}_c$ if we cannot find a better trajectory according to Def. 9. Otherwise, we fail (F) $\mathcal{X}_c$. We proceed as follows: We find the total violation scores of the rules in $\langle R, \sim_p, \leq_p \rangle$ for the candidate trajectory $\mathcal{X}_c$. If no rules in R are violated, then we pass the candidate trajectory. Otherwise, we investigate the existence of a better (less violating) trajectory. We take the middle of ego's current lane as the reference trajectory $\mathcal{X}_r$ and re-formulate the optimal control problem in (14) to recursively relax rules such that if the optimization is feasible, the generated trajectory is better than the candidate trajectory $\mathcal{X}_c$. Specifically, assume that the highest priority rule(s) that the candidate trajectory $\mathcal{X}_c$ violates belongs to $O_H, H \in \mathbb{N}$. Let $R_H \subseteq R_O$ denote the set of equivalence classes with priorities not larger than H, and $N_H \in \mathbb{N}$ denote the cardinality of R_H. We construct a power set $S_H = 2^{R_H}$, and then apply Alg. 1, in which we replace R_O by R_H.

Remark 3. *The procedure described above would fail a candidate trajectory $\mathcal{X}_c$ even if only a slightly better alternate trajectory (i.e., violating rules of the same highest priority but with slightly smaller violation scores) can be found by solving the optimal control problem. In practice, this might lead to an undesirably high failure rate. One way to deal with this, which we will consider in future work (see Sec. 7), is to allow for more classification categories, e.g., "Provisional Pass" (PP), which can then trigger further investigation of $\mathcal{X}_c$.*

Example 4. *Reconsider Exm. 2 and assume trajectory b is a candidate trajectory which violates rules r_2, r_4, thus, the highest priority rule that is violated by trajectory b belongs to O_2. We construct $R_H = \{O_1, O_2\}$. The power set $S_H = 2^{R_H}$ is then defined as $S_H = \{\{\emptyset\}, \{O_1\}, \{O_2\}, \{O_1, O_2\}\}$, and is sorted based on the total order as $S_{H_{sorted}} = \{\{\emptyset\}, \{O_1\}, \{O_2\}, \{O_1, O_2\}\}$.*

Algorithm 1: Recursive relaxation algorithm for finding optimal trajectory

Input: System (1) with $\boldsymbol{x}(0)$, cost function (7), control bound (2), state constraint (8), priority structure $\langle R, \sim_p, \leq_p \rangle$, reference trajectory $\mathcal{X}_r$

Output: Optimal ego trajectory and set of relaxed rules

1. Construct the power set of equivalence classes $S = 2^{R_O}$;
2. Sort the sets in S based on the highest priority of the equivalence classes in each set according to the total order and get $S_{sorted} = \{S_1, S_2, \ldots, S_{2^{N_O}}\}$;
3. $k = 0$;
while $k++ \leq 2^{N_O}$ **do**
  Solve (14) s.t. (1), (2), (11), (15), (16) and (17);
  if *the above problem is feasible for all* $t \in [0, T]$ **then**
    Generate the optimal trajectory $\mathcal{X}^*$ from (1);
    Construct relaxed set $R_{relax} = \{i : i \in O, O \in S_k\}$;
    if $\delta_i(t) = 0, \forall t \in [0, T]$ **then**
      Remove i from R_{relax};
    end
    break;
  end
end
4. Return $\mathcal{X}^*$ and R_{relax};

6 CASE STUDY

In this section, we apply the methodology developed in this paper to specific vehicle dynamics and various driving scenarios. Ego dynamics (1) are defined with respect to a reference trajectory [19], which measures the along-trajectory distance $s \in \mathbb{R}$ and the lateral distance $d \in \mathbb{R}$ of the vehicle Center of Gravity (CoG) with

respect to the closest point on the reference trajectory as follows:

$$\underbrace{\begin{bmatrix} \dot{s} \\ \dot{d} \\ \dot{\mu} \\ \dot{v} \\ \dot{a} \\ \dot{\delta} \\ \dot{\omega} \end{bmatrix}}_{\dot{\boldsymbol{x}}} = \underbrace{\begin{bmatrix} \frac{v\cos(\mu+\beta)}{1-d\kappa} \\ v\sin(\mu+\beta) \\ \frac{v}{l_r}\sin\beta - \kappa\frac{v\cos(\mu+\beta)}{1-d\kappa} \\ a \\ 0 \\ \omega \\ 0 \end{bmatrix}}_{f(\boldsymbol{x})} + \underbrace{\begin{bmatrix} 0 & 0 \\ 0 & 0 \\ 0 & 0 \\ 0 & 0 \\ 1 & 0 \\ 0 & 0 \\ 0 & 1 \end{bmatrix}}_{g(\boldsymbol{x})} \underbrace{\begin{bmatrix} u_{jerk} \\ u_{steer} \end{bmatrix}}_{\boldsymbol{u}}, \tag{18}$$

where μ is the vehicle local heading error determined by the difference of the global vehicle heading $\theta \in \mathbb{R}$ in (33) and the tangent angle $\phi \in \mathbb{R}$ of the closest point on the reference trajectory (i.e., $\theta = \phi + \mu$); v, a denote the vehicle linear speed and acceleration; δ, ω denote the steering angle and steering rate, respectively; κ is the curvature of the reference trajectory at the closest point; l_r is the length of the vehicle from the tail to the CoG; and u_{jerk}, u_{steer} denote the two control inputs for jerk and steering acceleration as shown in Fig. 5. $\beta = \arctan\left(\frac{l_r}{l_r+l_f}\tan\delta\right)$ where l_f is the length of the vehicle from the head to the CoG.

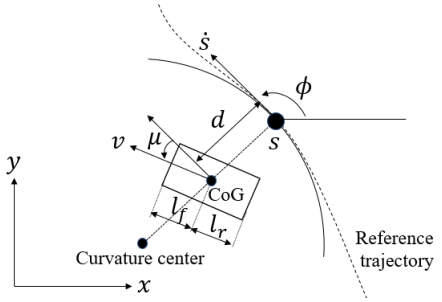


Figure 5: Coordinates of ego w.r.t a reference trajectory.

We consider the cost function in (14) as:

$$\min_{u_{jerk}(t),u_{steer}(t)} \int_0^T \left[u_{jerk}^2(t) + u_{steer}^2(t)\right] dt. \tag{19}$$

The reference trajectory $\mathcal{X}_r$ is the middle of ego's current lane, and is assumed to be given as an ordered sequence of points $\boldsymbol{p}_1$, $\boldsymbol{p}_2$, ..., $\boldsymbol{p}_{N_r}$, where $\boldsymbol{p}_i \in \mathbb{R}^2, i = 1, \ldots, N_r$ (N_r denotes the number of points). We can find the reference point $p_{i(t)}$, $i : [0, T] \to \{1, \ldots, N_r\}$ at time t as:

$$i(t) = \begin{cases} i(t)+1 & ||\boldsymbol{p}(t) - \boldsymbol{p}_{i(t)}|| \le \gamma, \\ j & \exists j \in \{1, 2, \ldots, N_r\} : ||\boldsymbol{p}(t) - \boldsymbol{p}_{i(t)}|| \ge ||\boldsymbol{p}(t) - \boldsymbol{p}_j||, \end{cases} \tag{20}$$

where $\boldsymbol{p}(t) \in \mathbb{R}^2$ denotes ego's location. $\gamma > 0$, and $i(0) = k$ for a $k \in \{1, 2, \ldots, N_r\}$ is chosen such that $||\boldsymbol{p}(0) - \boldsymbol{p}_j|| \ge ||\boldsymbol{p}(0) - \boldsymbol{p}_k||, \forall j \in \{1, 2, N_r\}$. Once we get $\boldsymbol{p}_{i(t)}$, we can update the progress s, the error states d, μ and the curvature κ in (18). The trajectory tracking in this case is to stabilize the error states d, μ ($\boldsymbol{y} = (d, \mu)$ in (11)) to 0, as introduced in Sec. 5.1. We also wish ego to achieve a desired speed $v_d > 0$ (otherwise, ego may stop in curved lanes). We achieve this by re-defining the CLF $V(\boldsymbol{x})$ in (11) as $V(\boldsymbol{x}) = ||\boldsymbol{y}||^2 + c_0(v - v_d)^2, c_0 > 0$. As the relative degree of $V(\boldsymbol{x})$ w.r.t. (18) is larger than 1, as mentioned in Sec. 5.1, we use input-to-state linearization and state feedback control [11] to reduce the relative degree to one [27]. For example, for the desired speed part in the CLF $V(\boldsymbol{x})$ ((18) is in linear form from v to u_{jerk}, so we don't need to do linearization), we can find a desired state feedback acceleration $\hat{a} = -k_1(v - v_d), k_1 > 0$. Then we can define a new CLF in the form $V(\boldsymbol{x}) = ||\boldsymbol{y}||^2 + c_0(a - \hat{a})^2 = ||\boldsymbol{y}||^2 + c_0(a + k_1(v - v_d))^2$ whose relative degree is just one w.r.t. u_{jerk} in (18). We proceed similarly for driving d, μ to 0 in the CLF $V(\boldsymbol{x})$ as the relative degrees of d, μ are also larger than one.

The control bounds (2) and state constraints (8) are given by:

$$\begin{aligned} &\text{speed constraint:} && v_{\min} \le v(t) \le v_{\max}, \\ &\text{acceleration constraint:} && a_{\min} \le a(t) \le a_{\max}, \\ &\text{jerk control constraint:} && u_{j,\min} \le u_{jerk}(t) \le u_{j,\max}, \\ &\text{steering angle constraint:} && \delta_{\min} \le \delta(t) \le \delta_{\max}, \\ &\text{steering rate constraint:} && \omega_{\min} \le \omega(t) \le \omega_{\max}, \\ &\text{steering control constraint:} && u_{s,\min} \le u_{steer}(t) \le u_{s,\max}, \end{aligned} \tag{21}$$

We consider the priority structure $\langle R, \sim_p, \leq_p \rangle$ from Fig. 6, with rules $R = \{r_1, r_2, r_3, r_4, r_5, r_6, r_7, r_8\}$, where r_1 is a pedestrian clearance rule; r_2 and r_3 are clearance rules for staying in the drivable area and lane, respectively; r_4 and r_5 are non-clearance rules specifying maximum and minimum speed limits, respectively; r_6 is a comfort non-clearance rule; and r_7 and r_8 are clearance rules for parked and moving vehicles, respectively. The formal rule definitions (statements, violation metrics) are given in Appendix A. These metrics are used to compute the scores for all the trajectories in the three scenarios below. The optimal disk coverage from Sec. 5.2 is used to compute the optimal controls for all the clearance rules, which are implemented using HOCBFs.

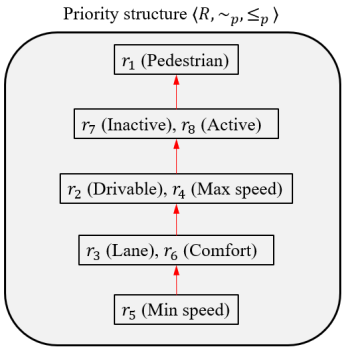


Figure 6: Priority structure for case study.

In the following, we consider three common driving scenarios in our tool (See Appendix C). For each of them, we solve the optimal control Problem 1 and perform pass/fail evaluation. In all three scenarios, in the pass/fail evaluation, an initial candidate trajectory is drawn "by hand" using the tool described in the Appendix. We use CLFs to generate a feasible trajectory $\mathcal{X}_c$ which tracks the candidate trajectory subject to the vehicle dynamics (1), control bounds (2) and state constraints (8).

6.1 Scenario 1

Assume there is an active vehicle, a parked (inactive) vehicle and a pedestrian, as shown in Fig. 7.

Optimal control: We solve the optimal control problem (14) by starting the rule relaxation from $S_1 = \{\emptyset\}$ (i.e., without relaxing any rules). This problem is infeasible in the given scenario since ego cannot maintain the required distance between both the active and the parked vehicles as the clearance rules are speed-dependent. Therefore, we relaxed the next lowest priority equivalence class set in S_{sorted}, i.e., the minimum speed limit rule in $S_2 = \{\{r_5\}\}$, for which we were able to find a feasible trajectory as illustrated in Fig. 7. By checking δ_i for r_5 from (14), we found it is positive in some time intervals in $[0, T]$, and thus, r_5 is indeed relaxed. The total violation score for rule r_5 from (26) for the generated trajectory is 0.539, and all other rules in R are satisfied. Thus, by Def. 10, the generated trajectory satisfies $\langle R, \sim_p, \leq_p \rangle$ in Fig. 6.

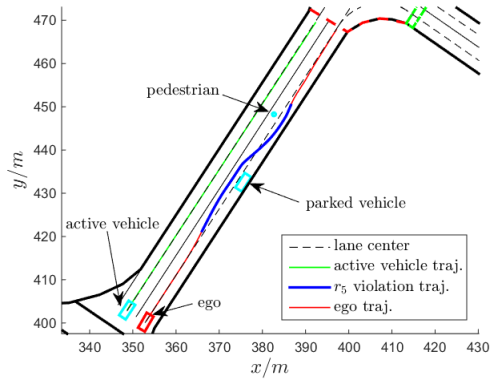


Figure 7: Optimal control for Scenario 1: the subset of ego trajectory violating r_5 is shown in blue.

Pass/Fail: The candidate trajectory $\mathcal{X}_c$ is shown in Fig. 8. This candidate trajectory only violates rule r_5 with total violation score 0.682. Following Sec. 5.4, we can either relax r_5 or do not relax any rules to find a possibly better trajectory. As shown in the above optimal control problem for this scenario, we cannot find a feasible solution if we do not relax rule r_5. Since the violation score of the candidate trajectory is larger than the optimal one, we fail this candidate trajectory.

6.2 Scenario 2

Assume there is an active vehicle, two parked (inactive) vehicles and two pedestrians, as shown in Fig. 9.

Optimal control: Similar to Scenario 1, the optimal control problem (14) starting from $S_1 = \{\emptyset\}$ (without relaxing any rules in R) is infeasible. We relax the next lowest priority rule set in S_{sorted}, i.e., the minimum speed rule in $S_2 = \{\{r_5\}\}$, for which we are able to find a feasible trajectory as illustrated in Fig. 9. Again, the δ_i for r_5 is positive in some time intervals in $[0, T]$, and thus, r_5 is indeed relaxed. The total violation score of the rule r_5 for the generated trajectory is 0.646, and all the other rules in R are satisfied.

Pass/Fail: The candidate trajectory $\mathcal{X}_c$ shown in red dashed line in Fig. 10 violates rules r_1, r_3 and r_8 with total violation scores 0.01, 0.23, 0.22 found from (22), (24),(29), respectively. In this scenario, we know that ego can change lane (where the lane keeping rule r_3 is in a lower priority equivalence class than r_1) to get reasonable trajectory. Thus, we show the case of relaxing the rules in the equivalence classes $O_2 = \{r_3, r_6\}$ and $O_1 = \{r_5\}$ to find a feasible trajectory that is better than the candidate one. The optimal control problem (14) generates a trajectory as the red-solid curve shown in Fig. 10, and only the δ_i for r_6 is 0 for all $[0, T]$. Thus, r_6 does not need to be relaxed. The generated trajectory violates rules r_3 and r_5 with total violation scores 0.124 and 0.111, respectively, but satisfies all the other rules including the highest priority rule r_1. According to Def. 9 for the given $\langle R, \sim_p, \leq_p \rangle$ in Fig. 6, the new generated trajectory is better than the candidate one, thus, we fail the candidate trajectory. Note that although this trajectory violates the lane keeping rule, it has a smaller violation score for r_5 compared to the trajectory obtained from the optimal control in Fig. 9 (0.111 v.s. 0.646), i.e., the average speed of ego in the red-solid trajectory in Fig. 10 is larger.

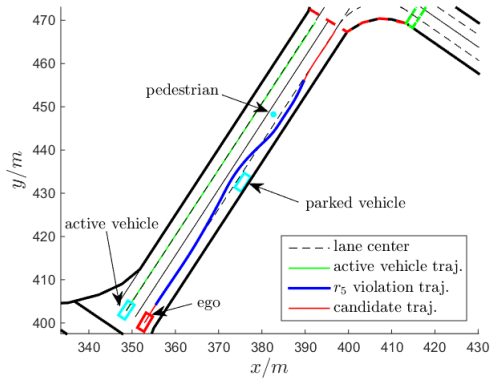


Figure 8: Pass/Fail for Scenario 1: the subset of the candidate trajectory violating r_5 is shown in blue.

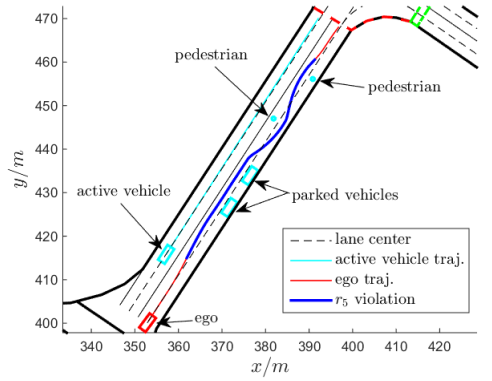


Figure 9: Optimal control for Scenario 2: the subset of ego trajectory violating r_5 is shown in blue.

6.3 Scenario 3

Assume there is an active vehicle, a parked vehicle and two pedestrians (one just gets out of the parked vehicle), as shown in Fig. 11.

Optimal control: Similar to Scenario 1, the optimal control problem (14) starting from $S_1 = \{\emptyset\}$ (without relaxing any rules in R) is infeasible. We relax the lowest priority rule set in S_{sorted}, i.e.,

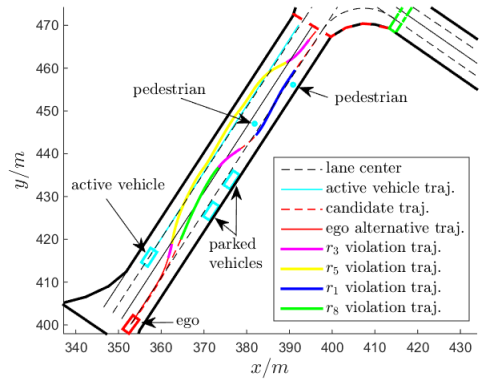


Figure 10: Pass/Fail for Scenario 2: the subsets of ego trajectory violating r_5, r_3 are shown in yellow and magenta, respectively; the subsets of the candidate trajectory violating r_8, r_3, r_1 are shown in green, magenta and blue, respectively.

the minimum speed rule $S_2 = \{\{r_5\}\}$, and solve the optimal control problem. In the (feasible) generated trajectory, ego stops before the parked vehicle, which satisfies all the rules in R except r_5. Thus, by Def. 10, the generated trajectory satisfies the priority structure $\langle R, \sim_p, \leq_p \rangle$. However, this might not be a desirable behavior, thus, we further relax the lane keeping r_3 and comfort r_6 rules and find the feasible trajectory shown in Fig. 11. δ_i for r_6 is 0 for all $[0, T]$, and, therefore, r_6 does not need to be relaxed. The total violation scores for the rules r_3 and r_5 are 0.058 and 0.359, respectively, and all other rules in R are satisfied.

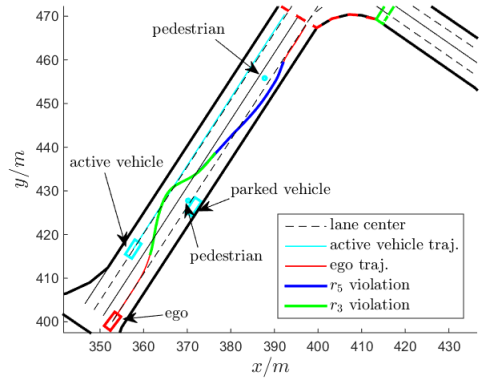


Figure 11: Optimal control for Scenario 3: the subsets of ego trajectory violating r_5, r_3 are shown in blue and green, respectively.

Pass/Fail: The candidate trajectory $\mathcal{X}_c$ shown as the red-dashed curve in Fig. 12 violates rules r_3 and r_8 with total violation scores 0.025 and 0.01, respectively. In this scenario, from the optimal control in Fig. 11 we know that ego can change lane (where the lane keeping rule is in a lower priority equivalence class than r_8). We show the case of relaxing the rules in the equivalence classes $O_2 = \{r_3, r_6\}$ and $O_1 = \{r_5\}$ (all have lower priorities than r_8). The optimal control problem (14) generates the red-solid curve shown in Fig. 12. By checking δ_i for r_6, we found that r_6 is indeed not relaxed. The generated trajectory violates rules r_3 and r_5 with total violation scores 0.028 and 0.742, respectively, but satisfies all other rules including r_8. According to Def. 9 and Fig. 6, the new generated trajectory (although violates r_3 more than the candidate trajectory, it does not violate r_8 which has a higher priority) is better than the candidate one. Thus, we fail the candidate trajectory.

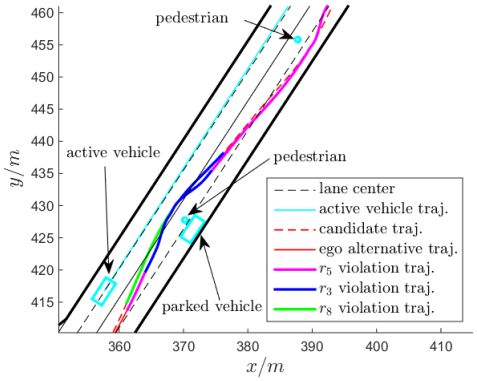


Figure 12: Pass/Fail for Scenario 3: the subsets of ego trajectory violating r_8, r_5, r_3 are shown in green, magenta and blue, respectively; the subsets of the candidate trajectory violating r_5, r_3 are shown in magenta and blue, respectively.

7 CONCLUSIONS AND FUTURE WORK

We developed a framework to design optimal control strategies for autonomous vehicles that are required to satisfy a set of traffic rules with a given priority structure, while following a reference trajectory and satisfying control and state limitations. We showed that, for commonly used traffic rules, by using control barrier functions and control Lyapunov functions, the problem can be cast as an iteration of optimal control problems, where each iteration involves a sequence of quadratic programs. We also showed that the proposed algorithms can be used to pass / fail possible autonomous vehicle behaviors against prioritized traffic rules. We presented multiple case studies for an autonomous vehicle with realistic dynamics and conflicting rules. Future work will be focused on learning priority structures from data, improving the feasibility of the control problems, and refinement of the pass / fail procedure.

REFERENCES

[1] A. D. Ames, K. Galloway, and J. W. Grizzle. 2012. Control Lyapunov Functions and Hybrid Zero Dynamics. In *Proc. of 51rd IEEE Conference on Decision and Control*. 6837–6842.

[2] A. D. Ames, X. Xu, J. W. Grizzle, and P. Tabuada. 2017. Control Barrier Function Based Quadratic Programs for Safety Critical Systems. *IEEE Trans. Automat. Control* 62, 8 (2017), 3861–3876.

[3] Z. Artstein. 1983. Stabilization with relaxed controls. *Nonlinear Analysis: Theory, Methods & Applications* 7, 11 (1983), 1163–1173.

[4] A. Censi, K. Slutsky, T. Wongpiromsarn, D. Yershov, S. Pendleton, J. Fu, and E. Frazzoli. 2019. Liability, Ethics, and Culture-Aware Behavior Specification using Rulebooks. In *2019 International Conference on Robotics and Automation*. 8536–8542.

[5] A. Collin, A. Bilka, S. Pendleton, and R. D. Tebbens. 2020. Safety of the Intended Driving Behavior Using Rulebooks. In *IV Workshop on Ensuring and Validating Safety for Automated Vehicles*. 1–7.

[6] R. Dimitrova, M. Ghasemi, and U. Topcu. 2018. Maximum realizability for linear temporal logic specifications. In *International Symposium on Automated Technology for Verification and Analysis*. 458–475.

[7] A. Donzé and O. Maler. 2010. Robust satisfaction of temporal logic over real-valued signals. In *International Conference on Formal Modeling and Analysis of Timed Systems*. 92–106.

[8] R. A. Freeman and P. V. Kokotovic. 1996. *Robust Nonlinear Control Design*. Birkhauser.

[9] P. Glotfelter, J. Cortes, and M. Egerstedt. 2017. Nonsmooth barrier functions with applications to multi-robot systems. *IEEE control systems letters* 1, 2 (2017), 310–315.

[10] ISO. 2019. PAS 21448-Road Vehicles-Safety of the Intended Functionality. *International Organization for Standardization* (2019).

[11] H. K. Khalil. 2002. *Nonlinear Systems*. Prentice Hall, third edition.

[12] L. Lindemann and D. V. Dimarogonas. 2019. Control barrier functions for signal temporal logic tasks. *IEEE Control Systems Letters* 3, 1 (2019), 96–101.

[13] O. Maler and D. Nickovic. 2004. Monitoring temporal properties of continuous signals. In *Proc. of International Conference on FORMATS-FTRTFT*. Grenoble, France, 152–166.

[14] N. Mehdipour, C. Vasile, and C. Belta. 2019. Arithmetic-geometric mean robustness for control from signal temporal logic specifications. In *American Control Conference*. 1690–1695.

[15] Q. Nguyen and K. Sreenath. 2016. Exponential Control Barrier Functions for Enforcing High Relative-Degree Safety-Critical Constraints. In *Proc. of the American Control Conference*. 322–328.

[16] M. Nolte, G. Bagschik, I. Jatzkowski, T. Stolte, A. Reschka, and M. Maurer. 2017. Towards a skill-and ability-based development process for self-aware automated road vehicles. In *2017 IEEE 20th International Conference on Intelligent Transportation Systems*. 1–6.

[17] M. Parseh, F. Asplund, M. Nybacka, L. Svensson, and M. Törngren. 2019. Pre-Crash Vehicle Control and Manoeuvre Planning: A Step Towards Minimizing Collision Severity for Highly Automated Vehicles. In *2019 IEEE International Conference of Vehicular Electronics and Safety (ICVES)*. 1–6.

[18] X. Qian, J. Gregoire, F. Moutarde, and A. D. L. Fortelle. 2014. Priority-based coordination of autonomous and legacy vehicles at intersection. In *IEEE conference on intelligent transportation systems*. 1166–1171.

[19] A. Rucco, G. Notarstefano, and J. Hauser. 2015. An Efficient Minimum-Time Trajectory Generation Strategy for Two-Track Car Vehicles. *IEEE Transactions on Control Systems Technology* 23, 4 (2015), 1505–1519.

[20] S. Shalev-Shwartz, S. Shammah, and A. Shashua. 2017. On a formal model of safe and scalable self-driving cars. *preprint in arXiv:1708.06374* (2017).

[21] K. P. Tee, S. S. Ge, and E. H. Tay. 2009. Barrier lyapunov functions for the control of output-constrained nonlinear systems. *Automatica* 45, 4 (2009), 918–927.

[22] J. Tmová, L. I R. Castro, S. Karaman, E. Frazzoli, and D. Rus. 2013. Minimum-violation LTL planning with conflicting specifications. In *2013 American Control Conference*. 200–205.

[23] S. Ulbrich and M. Maurer. 2013. Probabilistic online POMDP decision making for lane changes in fully automated driving. In *IEEE Conference on Intelligent Transportation Systems*. 2063–2067.

[24] L. Wang, A. D. Ames, and M. Egerstedt. 2017. Safety barrier certificates for collisions-free multirobot systems. *IEEE Transactions on Robotics* 33, 3 (2017), 661–674.

[25] R. Wisniewski and C. Sloth. 2013. Converse barrier certificate theorem. In *Proc. of 52nd IEEE Conference on Decision and Control*. Florence, Italy, 4713–4718.

[26] W. Xiao and C. Belta. 2019. Control Barrier Functions for Systems with High Relative Degree. In *Proc. of 58th IEEE Conference on Decision and Control*. Nice, France, 474–479.

[27] W. Xiao, C. Belta, and C. G. Cassandras. 2020. Adaptive Control Barrier Functions for Safety-Critical Systems. In *preprint in arXiv:2002.04577*.

[28] W. Xiao, C. Belta, and C. G. Cassandras. 2020. Feasibility Guided Learning for Constrained Optimal Control problems. In *Proc. of 59th IEEE Conference on Decision and Control*. 1896–1901.

APPENDIX

A RULE DEFINITIONS

Here we give definitions for the rules used in Sec. 6. According to Def. 7, each rule statement should be satisfied for all times.

r_1 : Maintain clearance with pedestrians

Statement: $d_{min,fp}(\boldsymbol{x}, \boldsymbol{x}_i) \geq d_1 + v(t)\eta_1, \forall i \in S_{ped}$

$$\varrho_{r,i}(\boldsymbol{x}(t)) = \max(0, \frac{d_1 + v(t)\eta_1 - d_{min,fp}(\boldsymbol{x}, \boldsymbol{x}_i)}{d_1 + v_{max}\eta_1})^2, \qquad (22)$$

$$\rho_{r,i}(\mathcal{X}) = \max_{t\in[0,T]} \varrho_{r,i}(\boldsymbol{x}(t)), \quad P_r = \sqrt{\frac{1}{n_{ped}} \sum_{i\in S_{ped}} \rho_{r,i}}.$$

where $d_{min,fp} : \mathbb{R}^{n+n_i} \to \mathbb{R}$ denotes the distance between footprints of ego and the pedestrian i, and the clearance threshold is given based on a fixed distance $d_1 \geq 0$ and increases linearly by $\eta_1 > 0$ based on ego speed $v(t) \geq 0$ (d_1 and η_1 are determined empirically), S_{ped} denotes the index set of all pedestrians, and $\boldsymbol{x}_i \in \mathbb{R}^{n_i}$ denotes the state of the pedestrian i. v_{max} is the maximum feasible speed of the vehicle and is used to define the normalization term in $\varrho_{r,i}$, which assigns a violation score (based on a L-2 norm) if formula is violated by $\boldsymbol{x}(t)$. $\rho_{r,i}$ defines the instance violation score as the most violating instant over $\mathcal{X}$. P_r aggregates the instance violations over all units (pedestrians), where $n_{ped} \in \mathbb{N}$ denotes the number of pedestrians.

r_2 : Stay in the drivable area

Statement: $d_{left}(\boldsymbol{x}(t)) + d_{right}(\boldsymbol{x}(t)) = 0$

$$\varrho_r(\boldsymbol{x}(t)) = \left(\frac{d_{left}(\boldsymbol{x}(t)) + d_{right}(\boldsymbol{x}(t))}{2d_{max}}\right)^2, \qquad (23)$$

$$\rho_r(\mathcal{X}) = \sqrt{\frac{1}{T}\int_0^T \varrho_r(\boldsymbol{x}(t))dt}, \quad P_r = \rho_r.$$

where $d_{left} : \mathbb{R}^n \to \mathbb{R}, d_{right} : \mathbb{R}^n \to \mathbb{R}$ denote the left and right infringement distances of ego footprint into the non-drivable areas, respectively. $d_{\max} > 0$ denotes the maximum infringement distance and is used to normalize the instantaneous violation score defined based on a L-2 norm, and ρ_r is the aggregation over trajectory duration T.

r_3 : Stay in lane

Statement: $d_{left}(\boldsymbol{x}(t)) + d_{right}(\boldsymbol{x}(t)) = 0$

$$\varrho_r(\boldsymbol{x}(t)) = \left(\frac{d_{left}(\boldsymbol{x}(t)) + d_{right}(\boldsymbol{x}(t))}{2d_{max}}\right)^2, \qquad (24)$$

$$\rho_r(\mathcal{X}) = \sqrt{\frac{1}{T}\int_0^T \varrho_r(\boldsymbol{x}(t))dt}, \quad P_r = \rho_r.$$

where $d_{left} : \mathbb{R}^n \to \mathbb{R}, d_{right} : \mathbb{R}^n \to \mathbb{R}$ denote the left and right infringement distances of ego footprint into the left and right lane boundaries, respectively, and violation scores are defined similar to

the rule r_2.

r_4 : Satisfy the maximum speed limit

Statement: $v(t) \leq v_{max,s}$

$$\varrho_r(\boldsymbol{x}(t)) = \max(0, \frac{v(t) - v_{max,s}}{v_{max}})^2, \qquad (25)$$
$$\rho_r(\mathcal{X}) = \sqrt{\frac{1}{T}\int_0^T \varrho_r(\boldsymbol{x}(t))dt}, \quad P_r = \rho_r.$$

where $v_{max,s} > 0$ denotes the maximum speed in a scenario s and varies for different road types (e.g., highway, residential, etc.).

r_5 : Satisfy the minimum speed limit

Statement: $v(t) \geq v_{min,s}$

$$\varrho_r(\boldsymbol{x}(t)) = \max(0, \frac{v_{min,s} - v(t)}{v_{min,s} - v_{min}})^2, \qquad (26)$$
$$\rho_r(\mathcal{X}) = \sqrt{\frac{1}{T}\int_0^T \varrho_r(\boldsymbol{x}(t))dt}, \quad P_r = \rho_r.$$

where $v_{min,s} > 0$ denotes the minimum speed in a scenario s which varies for different road types and $v_{min} > 0$ is the minimum feasible speed of the vehicle.

r_6 : Drive smoothly

Statement: $|a(t)| \leq a_{max,s} \wedge |a_{lat}(t)| \leq a_{lat,s}$

$$\varrho_r(\boldsymbol{x}(t)) = \left(\max(0, \frac{a_{max,s} - |a(t)|}{a_{max}}) + \max(0, \frac{a_{lat,s} - |a_{lat}(t)|}{a_{lat_m}})\right)^2,$$
$$\rho_r(\mathcal{X}) = \sqrt{\frac{1}{T}\int_0^T \varrho_r(\boldsymbol{x}(t))dt}, \quad P_r = \rho_r. \qquad (27)$$

where $a_{lat}(t) = \kappa v^2(t)$ denotes the lateral acceleration at time instant t; $a_{max,s} > 0$, $a_{lat,s} > 0$ denote the maximum and the allowed lateral acceleration in a scenario s, respectively; and a_{max} and $a_{lat_m} > 0$ denote the maximum feasible acceleration and maximum feasible lateral acceleration of the vehicle.

r_7 : Maintain clearance with parked vehicles

Statement: $d_{min,fp}(\boldsymbol{x}, \boldsymbol{x}_i) \geq d_7 + v(t)\eta_7, \forall i \in S_{pveh}$

$$\varrho_{r,i}(\boldsymbol{x}(t)) = \max(0, \frac{d_7 + v(t)\eta_7 - d_{min,fp}(\boldsymbol{x}, \boldsymbol{x}_i)}{d_7 + v_{max}\eta_7})^2, \qquad (28)$$
$$\rho_{r,i}(\mathcal{X}) = \max_{t\in[0,T]} \varrho_i(\boldsymbol{x}(t)), \quad P_r = \sqrt{\frac{1}{n_{pveh}}\sum_{i\in S_{pveh}} \rho_{r,i}}$$

where $d_{min,fp} : \mathbb{R}^{n+n_i} \to \mathbb{R}$ denotes the distance between footprints of ego and the parked vehicle i, $d_7 \geq 0$, $\eta_7 > 0$, and violation scores are defined similar to r_1, S_{pveh} and $n_{pveh} \in \mathbb{N}$ denote the index set and number of parked vehicles, respectively, and $\boldsymbol{x}_i \in \mathbb{R}^{n_i}$ denotes the state of the parked vehicle i.

r_8 : Maintain clearance with active vehicles

Statement: $d_{min,l}(\boldsymbol{x}, \boldsymbol{x}_i) \geq d_{8,l} + v(t)\eta_{8,l}$
$\wedge\ d_{min,r}(\boldsymbol{x}, \boldsymbol{x}_i) \geq d_{8,r} + v(t)\eta_{8,r}$
$\wedge\ d_{min,f}(\boldsymbol{x}, \boldsymbol{x}_i) \geq d_{8,f} + v(t)\eta_{8,f}, \forall i \in S_{aveh}$

$$\varrho_{r,i}(\boldsymbol{x}(t)) = \frac{1}{3}(\max(0, \frac{d_{8,l} + v(t)\eta_{8,l} - d_{min,l}(\boldsymbol{x}, \boldsymbol{x}_i)}{d_{8,l} + v_{max}\eta_{8,l}})^2$$
$$+ \max(0, \frac{d_{8,r} + v(t)\eta_{8,r} - d_{min,r}(\boldsymbol{x}, \boldsymbol{x}_i)}{d_{8,r} + v_{max}\eta_{8,r}})^2$$
$$+ \max(0, \frac{d_{8,f} + v(t)\eta_{8,f} - d_{min,f}(\boldsymbol{x}, \boldsymbol{x}_i)}{d_{8,f} + v_{max}\eta_{8,f}})^2),$$
$$\rho_{r,i}(\mathcal{X}) = \frac{1}{T}\int_0^T \varrho_{r,i}(\boldsymbol{x}(t))dt, \quad P_r = \sqrt{\frac{1}{n_{aveh} - 1}\sum_{i\in S_{aveh}\setminus ego} \rho_{r,i}} \qquad (29)$$

where $d_{min,l} : \mathbb{R}^{n+n_i} \to \mathbb{R}$, $d_{min,r} : \mathbb{R}^{n+n_i} \to \mathbb{R}$, $d_{min,f} : \mathbb{R}^{n+n_i} \to \mathbb{R}$ denote the distance between footprints of ego and the active vehicle i on the left, right and front, respectively; $d_{8,l} \geq 0, d_{8,r} \geq 0, d_{8,f} \geq 0, \eta_{8,l} > 0, \eta_{8,r} > 0, \eta_{8,f} > 0$ are defined similarly as in r_1, and S_{aveh} and $n_{aveh} \in \mathbb{N}$ denote the index set and number of active vehicles, and $\boldsymbol{x}_i \in \mathbb{R}^{n_i}$ denotes the state of the active vehicle i. Similar to Fig. 3, we show in Fig. 13 how r_8 is defined based on the clearance region and optimal disk coverage proposed in Sec. B.

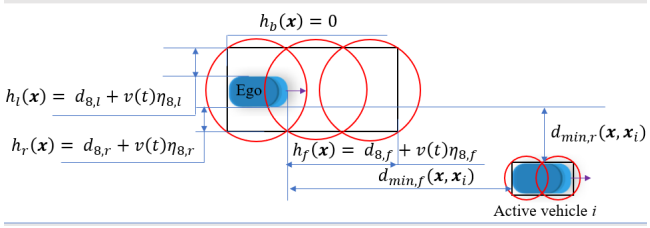


Figure 13: Formulation of r_8 with the optimal disk coverage approach: r_8 is satisfied since clearance regions of ego and the active vehicle $i \in S_p$ do not overlap.

B OPTIMAL DISK COVERAGE

To construct disks to fully cover the clearance regions, we need to find their number and radius. From Fig. 4, the lateral approximation error $\sigma > 0$ is given by:

$$\sigma = \mathfrak{r} - \frac{w + h_l(\boldsymbol{x}) + h_r(\boldsymbol{x})}{2}. \qquad (30)$$

Since σ for ego depends on its state $\boldsymbol{x}$ (speed-dependent), we consider the accumulated lateral approximation error for all possible $\boldsymbol{x} \in X$. This allows us to determine z and $\mathfrak{r}$ such that the disks fully cover ego clearance region for all possible speeds in $\boldsymbol{x}$. Let $\bar{h}_i = \sup_{\boldsymbol{x}\in X} h_i(\boldsymbol{x}), \underline{h}_i = \inf_{\boldsymbol{x}\in X} h_i(\boldsymbol{x}), i \in \{f, b, l, r\}$. We can formally formulate the construction of the approximation disks as an optimization problem:

$$\min_z z + \beta \int_{\underline{h}_f}^{\bar{h}_f} \int_{\underline{h}_b}^{\bar{h}_b} \int_{\underline{h}_l}^{\bar{h}_l} \int_{\underline{h}_r}^{\bar{h}_r} \sigma dh_f(\boldsymbol{x}) dh_b(\boldsymbol{x}) dh_l(\boldsymbol{x}) dh_r(\boldsymbol{x}) \qquad (31)$$

subject to

$$z \in \mathbb{N}, \tag{32}$$

where $\beta \geq 0$ is a trade-off between minimizing the number of the disks (so as to minimize the number of constraints considered with CBFs) and the coverage approximation error. The above optimization problem is solved offline. A similar optimization is formulated for construction of disks for instances in S_p (we remove the integrals due to speed-independence). Note that for the driving scenarios studied in this paper, we omit the longitudinal approximation errors in the front and back. The lateral approximation errors are considered in the disk formulation since they induce conservativeness in the lateral maneuvers of ego required for surpassing other instances (such as parked car, pedestrians, etc.), see Sec. 6.

Let $(x_e, y_e) \in \mathbb{R}^2$ be the center of ego and $(x_i, y_i) \in \mathbb{R}^2$ be the center of the instance $i \in S_p$. The center of the disk j for ego $(x_{e,j}, y_{e,j}), j \in \{1, \ldots, z\}$ is determined by:

$$\begin{aligned} x_{e,j} &= x_e + \cos\theta_e(-\frac{l}{2} - h_b(\boldsymbol{x}) + \frac{l + h_f(\boldsymbol{x}) + h_b(\boldsymbol{x})}{2z}(2j-1)) \\ y_{e,j} &= y_e + \sin\theta_e(-\frac{l}{2} - h_b(\boldsymbol{x}) + \frac{l + h_f(\boldsymbol{x}) + h_b(\boldsymbol{x})}{2z}(2j-1)) \end{aligned} \tag{33}$$

where $j \in \{1, \ldots, z\}$ and $\theta_e \in \mathbb{R}$ denotes the heading angle of ego. The center of the disk k for the instance $i \in S_p$ denoted by $(x_{i,k}, y_{i,k}), k \in \{1, \ldots, z_i\}$ can be defined similarly.

Theorem 3. *If the clearance regions of ego and the instance $i \in S_p$ are covered by the disks constructed by solving (31), then satisfaction of (13) implies non-overlapping of the clearance regions between ego and the instance i.*

Proof. Consider z and z_i disks with minimum radius $\mathfrak{r}$ and $\mathfrak{r}_i$ from (12) associated with clearance region of ego and instance $i \in S_p$, respectively. The constraints in (13) guarantee that there is no overlap of the disks between the vehicle $i \in S_p$ and instance $j \in S_p$. Since the clearance regions are fully covered by these disks, we conclude that the clearance regions do not overlap. □

C SOFTWARE TOOL AND SIMULATION PARAMETERS

We implemented the computational procedure described in this paper as a user-friendly software tool in Matlab. The tool allows to load a map represented by a .json file and place vehicles and pedestrians on it. It provides an interface to generate smooth reference / candidate trajectories and it implements our proposed optimal control and P/F frameworks; the *quadprog* optimizer was used to solve the QPs (solve time $< 0.01s$ for each QP) and $ode45$ to integrate the vehicle dynamics (18). All the computation in this paper was performed on a Intel(R) Core(TM) i7-8700 CPU @ 3.2GHz×2.

The simulation parameters are considered as follows: $v_{max} = 10m/s, v_{min} = 0m/s, a_{max} = -a_{min} = 3.5m/s^2, u_{j,max} = -u_{j,min} = 4m/s^3, \delta_{max} = -\delta_{min} = 1rad, \omega_{max} = -\omega_{min} = 0.5rad/s, u_{s,max} = -u_{s,min} = 2rad/s^2, w = 1.8m, l = 4m, l_f = l_r = 2m, d_1 = 1m, \eta_1 = 0.067s, v_{max,s} = 7m/s, v_{min,s} = 3m/s, a_{max,s} = 2.5m/s^2, a_{lat_m} = 3.5m/s^2, a_{lat,s} = 1.75m/s^2, d_7 = 0.3m, \eta_7 = 0.13s, d_{8,l} = d_{8,r} = 0.5m, d_{8,f} = 1m, \eta_{8,r} = \eta_{8,l} = 0.036s, \eta_{8,f} = 2s, v_d = 4m/s, \beta = 2$ in (31).